

Research Article

Mesoporous $(\text{Ta}, \text{Nb})_3\text{W}_7$ Modified with Stearic Acid Used as Solid Acids for Esterification

Fei Chang,^{1,2} Rui Wang,³ Quan Zhou,¹ Hu Pan,¹ and Heng Zhang¹

¹Center for Research and Development of Fine Chemicals, State-Local Joint Laboratory for Comprehensive Utilization of Biomass, State Key Laboratory Breeding Base of Green Pesticide and Agricultural Bioengineering, Ministry of Education, Guizhou University, Guiyang 550025, China

²Institute of Comprehensive Utilization of Plant Resources, Kaili College, Kaili 556011, China

³Food and Pharmaceutical Engineering Institute, Guiyang College, Guiyang 550005, China

Correspondence should be addressed to Fei Chang; feichang1980@126.com

Received 29 November 2016; Revised 5 February 2017; Accepted 15 February 2017; Published 7 March 2017

Academic Editor: Oluwafunmilola Ola

Copyright © 2017 Fei Chang et al. This is an open access article distributed under the Creative Commons Attribution License, which permits unrestricted use, distribution, and reproduction in any medium, provided the original work is properly cited.

Mesoporous solid acids Ta_3W_7 and Nb_3W_7 were prepared from TaCl_5 and NbCl_5 with WCl_6 in the presence of stearic acid (SA) via a sol-gel method, respectively. For comparison, mesoporous Ta_3W_7 -P123 mixed oxides and mesoporous Nb_3W_7 -P123 mixed oxides were synthesized in the same way. The catalysts were characterized through TGA, XRD, SEM, TEM, BET, and NH_3 -TPD. Experimental results showed that Ta_3W_7 -SA and Nb_3W_7 -SA exhibited several advantages such as higher activity, shorter preparation period, lower cost, stronger acid sites, and higher surface area, which had potential to be used as mesoporous heterogeneous catalysts in biodiesel production.

1. Introduction

Finding an environment-friendly, green, and sustainable energy to substitute fuel has become an urgent issue in the today's world [1]. Biodiesel, a biodegradable and renewable form of energy, consisting of mono alkyl esters of fatty acids derived from sources such as vegetable oils and animal fats, has cardinal potential as alternative fuels [2]. Typically, preparation of the biodiesel includes esterification and transesterification, each of which also includes homogeneous and heterogeneous catalytic process. The heterogeneous catalysis concerned simple separation, reusable, low-cost, and environmentally friendly advantages compared to the homogeneous catalysis. Among them, the solid base-mediated process is one of the most commercially useable methods in transesterification to produce biodiesel under mild reaction conditions with high efficiency, but it is quite limited for high acidic oils, CO_2 , and H_2O , and outflow of the catalyst is serious. In contrast, the solid acid catalyst is more effective for converting high free fatty acids (FFA) although harsh reaction conditions (high reaction temperature, long

reaction time, relatively high pressure, and high alcohol-oil ratio) are required in esterification [3–5]. Therefore, acid-catalyzed esterification combined with alkali-catalyzed transesterification of feedstocks having high FFA contents has been developed for biodiesel production [6–9].

Tagusagawa et al. [10, 11] investigated the solid acids $\text{Nb}_x\text{Mo}_{10-x}$ and $\text{Nb}_x\text{W}_{10-x}$ mixed oxides prepared using a poly block copolymer surfactant pluronic P-123 by a sol-gel method for biodiesel production. When the molar ratio of Nb/Mo and Nb/W was 3 : 7, the catalysts exhibited the highest catalytic activity in esterification. However, the templating agent P123 is rather expensive and the period of the catalyst preparation is quite long (14 days).

In 2013, we investigated the natural calcite and dolomite modified with stearic acid via simple thermal decomposition of the reaction mixtures for preparing a series of solid base catalysts. It was demonstrated that the solid base catalysts modified with the templating agents-stearic acid (SA) were environmentally friendly and displayed high catalytic activity for transesterification reactions. The highly efficient catalysts had the high special surface areas and base site densities. In

addition, the mixed-oxide catalysts could be reused several times without significant loss of catalytic activity [12].

In this study, we used SA and P-123 as template to modify the Ta-W and Nb-W mixed oxides, separately synthesizing mesoporous solid acid catalysts Ta₃W₇-SA and Nb₃W₇-SA. The as-prepared catalysts were characterized by XRD, SEM, TEM, BET, and NH₃-TPD. Besides, the activity of the prepared catalysts was assessed for three high acid value plants oils (*Euphorbia lathyris* L., *Sapium sebiferum* L., and *Jatropha curcas* L.) in esterification reaction. The formation of acidic sites on the catalysts was investigated via the Hammett indicator method, and the optimized reaction conditions were also carried out.

2. Experimental

2.1. Materials. Analytical reagent-grade stearic acid (>99%), methanol, and other agents were purchased from Kermel Chemical Reagent Co., Ltd., Tianjing, China; NbCl₅ (>99.9%), WCl₆ (>99.9%) and TaCl₅ (>99.9%) were purchased from Aladdin Industrial Corporation, Shanghai, china; JCO and ELO were obtained by squeezing *Jatropha curcas* L. and *Euphorbia lathyris* L. seeds obtained from Luodian County, Guizhou Province, and Bozhou City, Anhui Province, China. DSSKO was prepared from *Sapium sebiferum* L. oil purchased from Suizhou Tianfeng Local Product Co., Ltd. (Suizhou, China).

2.2. Catalyst Preparation. Mesoporous Ta₃W₇-P123 mixed oxides: 1.00 g P-123 was added to 10.00 g anhydrous *n*-propanol and stirred for 0.5 h. To the stirring solution of anhydrous alcohol, 0.0018 mol NbCl₅ and 0.0042 mol WCl₆ (total chloride: 0.06 mmol) were added; then 30 mmol distilled water was added and stirred for another 0.5 h. The resulting solution was placed in a porcelain boat for 14 days at 40°C. The product was calcined in a tube furnace in air flow rate of 40 L/h, 1°C/min heating to 600°C. When the temperature was raised to 600°C, air was stopped and incubated for 5 h at 600°C.

Mesoporous Nb₃W₇-P123 mixed oxides: same method was used to prepare mesoporous Ta₃W₇-SA mixed oxides by changing the raw materials.

Mesoporous Ta₃W₇-SA mixed oxides: 0.03 mol TaCl₅, 0.07 mol WCl₆, and 162.36 g SA were blended and stirred for 3 h at 170°C; the hot mixture was poured into a porcelain boat and calcined according to the method for preparation of mesoporous Ta₃W₇-P123 mixed oxides.

Mesoporous Nb₃W₇-SA mixed oxides: same method was utilized as that for preparation of mesoporous Ta₃W₇-SA mixed oxides with corresponding precursors.

2.3. Catalyst Characterization

2.3.1. TGA. The catalysts were calcined in high-purity nitrogen (99.999 wt.%, 100 mL/min) at 4°C/min of the heating rate within the range of 35–750°C.

2.3.2. X-Ray Diffraction Analysis. To determine the crystal structure, the catalysts were studied by the Bruker D8 Advanced X-ray diffractometer with Cu K α radiation (λ = 0.154 nm) at 40 kV and 30 mA with a step size of 0.02.

2.3.3. SEM. The surface morphology of the catalysts was characterized via FEI inspect f 50 type scanning electron microscope; the catalysts were taken after being dried and ground, then placed on the processing stations, and tested.

2.3.4. TEM. The internal structure of catalysts was analyzed by FEI Tecnai G2 F20 S-TWIN 200 kV transmission electron microscope. The samples were dried, ground, and dispersed in the ethanol, then added dropwise on the coated copper mesh, and dried in vacuo to subject TEM analysis.

2.3.5. N₂ Adsorption-Desorption. The pore size distribution (Barrett-Joyner-Halenda method), the specific surface area (P/P_0 = 0.05 to 0.20), and pore volume (relative pressure of about 0.99) of the catalysts were measured by a Micromeritics TriStar II 3020 system (adsorption of N₂ at 77 K) and the catalysts were degassed at 300°C for 3 h.

2.3.6. NH₃-TPD. The catalysts' relative acid site intensity and distribution were obtained by using an AutoChem 2920 chemisorption analyzer.

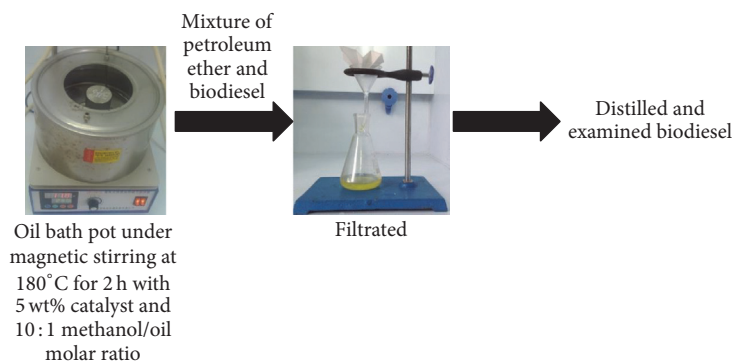
2.4. Catalytic Activity for Esterification. The amount of JCO, ELO, and DSSKO was weighted and added to the autoclave, respectively. Then, a certain amount of methanol and catalyst was mixed into above oil. The autoclave was installed and put into the oil bath pot with magnetic stirring apparatus, after a period of time of reaction, an appropriate amount of petroleum ether was added to the reaction mixture, shaken up, and filtrated, and the filtrate was distilled under reduced pressure (Scheme 1). The acid value of the base oil and esterified oil was examined via the method of the ISO 660-1996. The conversion rate of FFA was counted by the following formula [13, 14]:

$$\text{FFA conversion (wt.\%)} = \frac{\text{initial acid value} - \text{final acid value}}{\text{initial acid value}} \quad (1)$$

3. Results and Discussion

3.1. Catalyst Characterization

3.1.1. Thermal Stability. The mesoporous Nb₃W₇ oxide (P-123), mesoporous Ta₃W₇ oxide (P-123), mesoporous Nb₃W₇ oxide (stearic acid), and mesoporous Ta₃W₇ oxide (stearic acid) were analyzed by TGA (Figure 1), separately. The weightlessness of mesoporous Nb₃W₇ oxide (P-123) and Ta₃W₇ oxide (P-123) occurred at 200°C mainly; the weightlessness value was 42.61 wt% and 35.03 wt%, respectively. But, the weight loss of mesoporous Nb₃W₇ and Ta₃W₇ oxide (stearic acid) was 84.56 wt% and 88.86 wt% at 400°C, respectively. Furthermore, these four catalysts showed no significant weight loss at 400–750°C. Thus, the catalysts were calcined with an air flow rate of 40 L/h in the tube furnace and the temperature was raised to 600°C with 1°C/min (maintained at this temperature for 300 min).



SCHEME 1: Reaction schematic for biodiesel production.

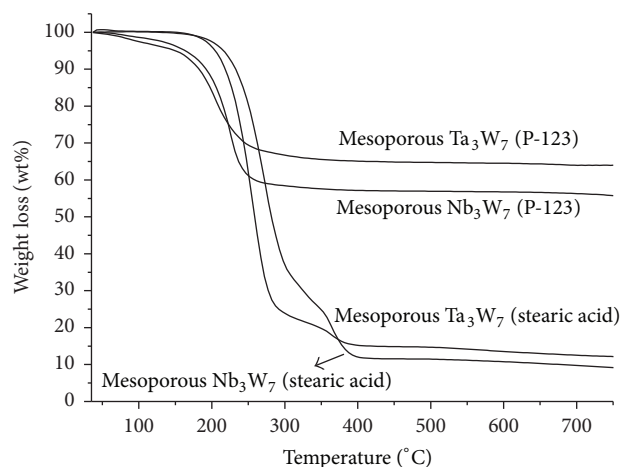
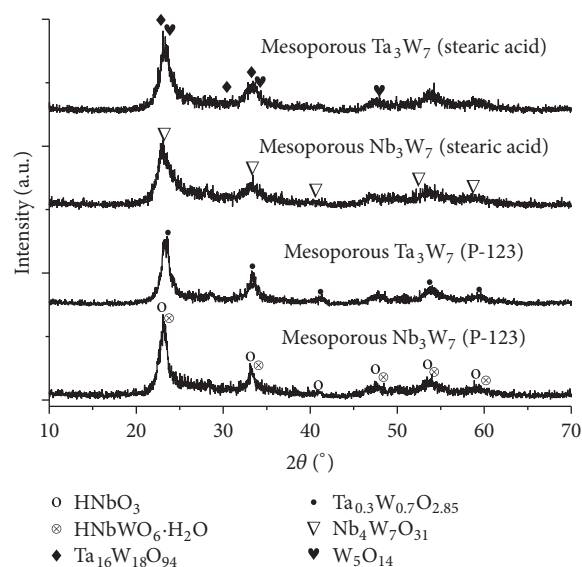


FIGURE 1: TGA curves for precursors of catalysts.

3.1.2. Crystal Structure. Wide-angle diffraction patterns of mesoporous Nb_3W_7 oxide (stearic acid), mesoporous Ta_3W_7 oxide (stearic acid), and $\text{Nb}_2\text{O}_5\text{-WO}_3$ and $\text{Ta}_2\text{O}_5\text{-WO}_3$ were obtained by XRD detection (Figure 2). As seen from Figure 2, the catalysts were amorphous. The weak and broad diffraction peaks demonstrated that the catalysts had typical characteristics of nanoparticles and surface species, indicating that the catalysts were more uniform. Taking the mesoporous Ta_3W_7 oxide (stearic acid) as an example, the surface diffraction peaks of the catalyst could be attributed to $\text{Ta}_{16}\text{W}_{18}\text{O}_{94}$ (22.86° , 33.27° , and 30.43°) and W_5O_{14} (23.37° , 34.06° , and 47.88°).

3.1.3. Scanning Electron Microscopy (SEM). Figure 3 shows the SEM image of the mesoporous Ta_3W_7 oxide (stearic acid) catalyst. The sample formed an uneven surface due to the accumulation of small particles. Part of the holes formed makes the catalyst have more active sites to improve the catalytic activity. Moreover, the sample surface was uniform, as it could be obtained from Figure 3(b).

3.1.4. Transmission Electron Microscopy (TEM). In order to obtain structural characteristics of the mesoporous Ta_3W_7 oxide (stearic acid) catalyst, the sample was characterized via

FIGURE 2: Wide-angle diffraction patterns of mesoporous Nb_3W_7 oxide (P-123), mesoporous Ta_3W_7 oxide (P-123), mesoporous Nb_3W_7 oxide (stearic acid), and mesoporous Ta_3W_7 oxide (stearic acid).

the transmission electron microscopy (TEM). It can be seen from Figure 4(a) that uniform mesoporous one-dimensional pore structure and existing grooves were generated on the surface of the sample. Therefore, the structure resulted in a large specific surface area for the catalyst [15]; the result was consistent with N_2 adsorption-desorption and pore size distribution analysis (Figures 5 and 7). Moreover, uniform particle size (10–15 nm) was shown in Figure 4(b) and the agglomeration was not found.

3.1.5. Specific Surface Area (SSA) and Pore Size Distribution Analysis. The N_2 adsorption/desorption isotherms and pore size distribution curves for this series of solid acid catalysts were shown in Figures 5–7. The specific surface area, the average pore diameter, and pore volume data of the catalysts were showed in Table 1. As seen from Figure 5, five catalysts possessed IV adsorption isotherm of H1-type hysteresis loop, and the isotherms became flatten at the strong pressure area

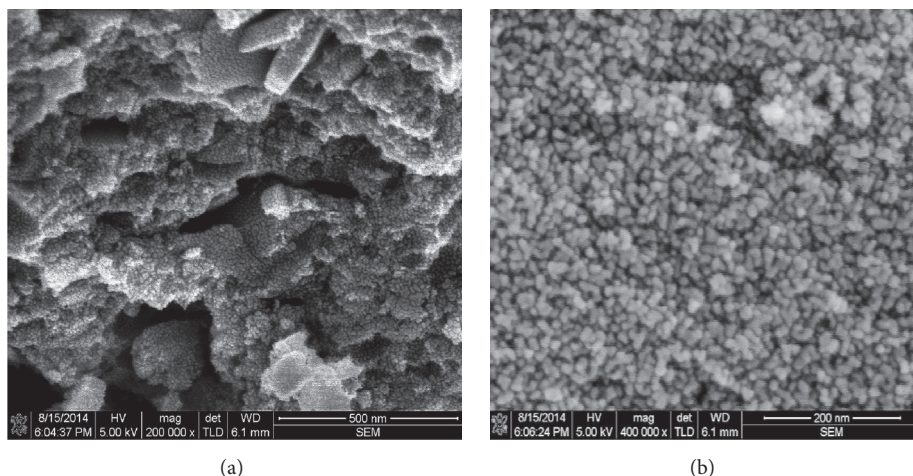


FIGURE 3: SEM images of mesoporous Ta_3W_7 oxide (stearic acid).

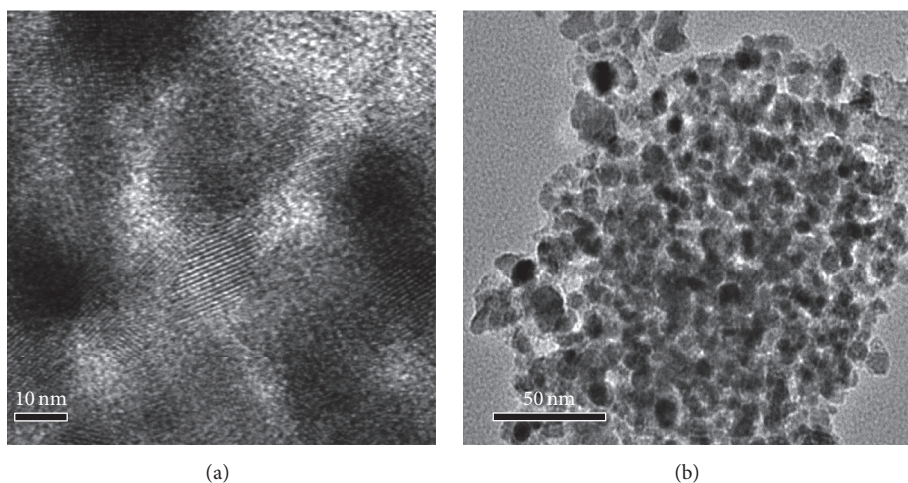


FIGURE 4: TEM images of mesoporous Ta_3W_7 oxide (stearic acid).

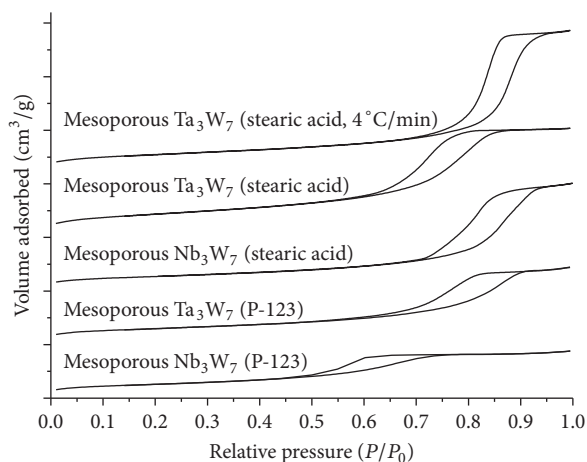


FIGURE 5: N_2 adsorption-desorption isotherms of mesoporous Nb_3W_7 oxide (P-123), mesoporous Ta_3W_7 oxide (P-123), mesoporous Nb_3W_7 oxide (stearic acid), mesoporous Ta_3W_7 oxide (stearic acid), and mesoporous Ta_3W_7 oxide (stearic acid, $4^\circ\text{C}/\text{min}$).

(P/P_0). It was shown that these catalysts had uniform mesoporous pore size distribution [16], which was consistent with the pore size distribution curves (Figures 6 and 7). Among the five catalysts, the calcination with the heating rate of $1^\circ\text{C}/\text{min}$ processed Ta_3W_7 oxide (stearic acid) showed the largest SSA ($107.49\text{ m}^2/\text{g}$, Table 1). But, the SSA of Ta_3W_7 oxide (stearic acid, $4^\circ\text{C}/\text{min}$) was only $86.27\text{ m}^2/\text{g}$. In addition, the closing point of hysteresis loop of the mesoporous Ta_3W_7 oxide (stearic acid, $4^\circ\text{C}/\text{min}$) moved to high P/P_0 compared with the mesoporous Ta_3W_7 oxide (stearic acid, $1^\circ\text{C}/\text{min}$, Figure 5). It was inferred that the pore size of the mesoporous Ta_3W_7 oxide (stearic acid, $4^\circ\text{C}/\text{min}$) was larger, and this result could be verified from Figure 6.

3.1.6. Acidity. The mesoporous Ta_3W_7 oxide (P-123) and mesoporous Ta_3W_7 oxide (stearic acid) were tested by NH_3 -TPD to explain the relationship between the chemical properties of solid acid catalysts and catalytic properties. Figure 8 demonstrated that the mesoporous Ta_3W_7 oxide

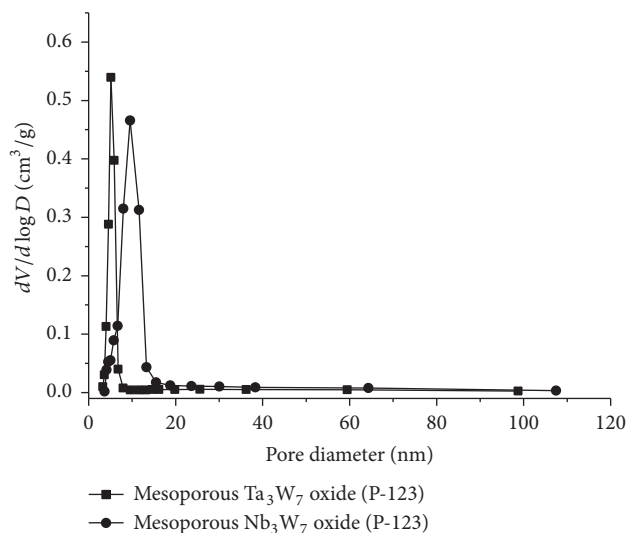


FIGURE 6: BJH pore size distributions of mesoporous Nb_3W_7 oxide (P-123) and mesoporous Ta_3W_7 oxide (P-123).

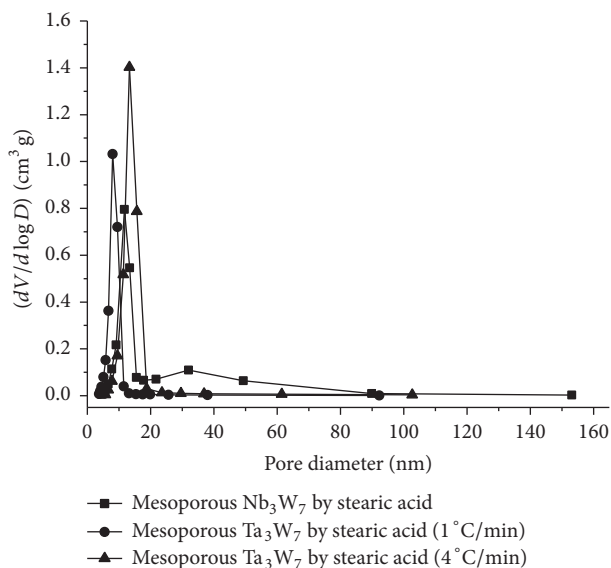


FIGURE 7: BJH pore size distributions of mesoporous Nb_3W_7 oxide (stearic acid), mesoporous Ta_3W_7 oxide (stearic acid, $1^\circ\text{C}/\text{min}$), and mesoporous Ta_3W_7 oxide (stearic acid, $4^\circ\text{C}/\text{min}$).

(stearic acid) and mesoporous Ta_3W_7 oxide (P-123) showed not only NH_3 desorption peak in the vicinity of 170°C , but also desorption peak at 800°C high temperature nearby. It was illustrated that these two kinds of samples had two different acid sites, and the appearance of NH_3 desorption peak at 800°C meant high acid strength. It was proposed that the high valence of W_6^{+} and low valence of Ta_5^{+} could produce strong Bronsted acidic sites for the between ions of isomorphic substitution effect [10, 11]. The acid site density of the mesoporous Ta_3W_7 oxide (stearic acid, 1.233 mmol/g) was larger than that of the mesoporous Ta_3W_7 oxide (P-123, 0.347 mmol/g) from the NH_3 -TPD too. This result illustrated

that the catalytic active sites were greatly connected with the preparation method of the catalyst when the elements were the same.

3.2. Esterification

3.2.1. Catalytic Performances of Different Catalysts. The catalytic performances of the Nb_2O_5 , Ta_2O_5 , WO_3 , $\text{Nb}_2\text{O}_5\text{-WO}_3$, $\text{Ta}_2\text{O}_5\text{-WO}_3$ [17], mesoporous Nb_3W_7 oxide (P-123), mesoporous Ta_3W_7 oxide (P-123), mesoporous Nb_3W_7 oxide (stearic acid), and mesoporous Ta_3W_7 oxide (stearic acid, $1^\circ\text{C}/\text{min}$) were investigated under the identical conditions: the amount of catalyst 5 wt%, methanol to oil molar ratio of 8:1 and at 180°C for 1 h, respectively, and the catalytic activity of the above catalysts were evaluated via FFA conversion rate (Figure 9).

The results showed that the mesoporous Ta_3W_7 oxide (stearic acid, $1^\circ\text{C}/\text{min}$) exhibited the best activity in esterification. Although SSA of the mesoporous Nb_3W_7 oxide (stearic acid) was almost the same as the mesoporous Ta_3W_7 oxide (P-123) and the former was only one-third of the latter with the density of active sites, the esterification activity of the mesoporous Nb_3W_7 oxide (stearic acid) exceeded the mesoporous Ta_3W_7 oxide (P-123). The performance of catalyst was deduced to be affected by the active site density, strength, and physical structure [18, 19].

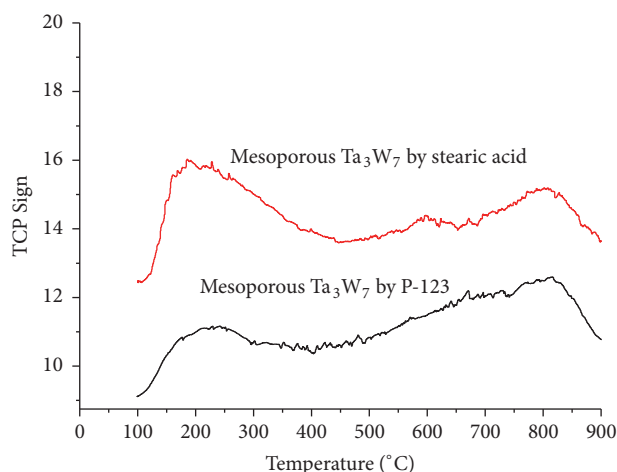
3.2.2. Single Factor Optimization. In this study, the high acid value *Jatropha* oil (25.41 mg KOH/g) was used as the feed oil, which is quite high in relative to the natural vegetable oils [20]. Single factor (methanol/oil molar ratio, reaction time, and reaction temperature) of the mesoporous Ta_3W_7 oxide (stearic acid, $1^\circ\text{C}/\text{min}$) was optimized with 5 wt.% catalyst loading.

(1) Methanol/Oil Molar Ratio. 5 wt.% mesoporous Ta_3W_7 oxide (stearic acid, $1^\circ\text{C}/\text{min}$) was added to the molar ratio of methanol to oil of 8:1, 10:1, and 12:1 at 180°C for 1 h, respectively. The FFA conversion rate was used as the standard to measure the catalytic activity of the catalyst, and the results are illustrated in Figure 10. When the methanol to oil molar ratio was 8:1, the FFA conversion rate reached 70.43%, and when the molar ratio of methanol to oil increased to 10:1, 72.76% of the FFA conversion rate was attained. But, with further enhancing the methanol to oil molar ratio to 12:1, the FFA conversion rate was not improved significantly.

(2) Reaction Temperature. Kulkarni et al. [21] found that the polymerization reaction would occur as the unsaturated fatty oils acids of the animal and vegetable fats were heating at a temperature above 225°C . Therefore, the reaction temperature was selected at 160°C , 180°C , and 200°C respectively, and the catalysts in an amount of 5 wt.% and 10:1 methanol/oil ratio were used to investigate the catalytic activity of the mesoporous Ta_3W_7 oxide (stearic acid, $1^\circ\text{C}/\text{min}$). As seen from Figure 11, without considering the amount of catalyst, impact of the reaction temperature is great for the mesoporous Ta_3W_7 oxide (stearic acid, $1^\circ\text{C}/\text{min}$). The FFA conversion rate was 51.29% at 160°C ; however, when the

TABLE 1: Physicochemical properties of catalyst samples.

Catalyst	SSA (m ² /g)	Average pore diameter (nm)	Pore volume (cm ³ /g)	Crystal size (nm)
Mesoporous Nb ₃ W ₇ oxide (P-123)	73.09	8.34	0.11	11.18
Mesoporous Ta ₃ W ₇ oxide (P-123)	64.09	5.1	0.07	10.02
Mesoporous Nb ₃ W ₇ oxide (stearic acid, 1°C/min)	66.12	11.8	0.18	12.53
Mesoporous Ta ₃ W ₇ oxide (stearic acid, 1°C/min)	107.49	7.33	0.16	11.88
Mesoporous Ta ₃ W ₇ oxide (stearic acid, 4°C/min)	86.27	12.91	0.21	13.97

FIGURE 8: NH₃-TPD curves of mesoporous Ta₃W₇ oxide (P-123) and mesoporous Ta₃W₇ oxide (stearic acid).

temperature was raised to 180°C, the FFA conversion rate reached 72.61%. If the temperature rose to 200°C, the FFA conversion rate had no significant improvement; moreover, the color of the product became darker.

(3) *Reaction Time*. The reaction time (1, 2, and 3 h) was studied on the basis of the above optimal reaction conditions (methanol/oil molar ratio and reaction temperature). The optimum reaction time of 2 h was determined from Figure 12. Extension of the reaction time did not improve the FFA conversion rate significantly because the esterification reaction was a reversible equilibrium; when the reaction of H₂O in the system reached a certain content, the reaction was difficult to carry out the forward reaction.

Through a series of single factor experiments, the optimal conditions of the mesoporous Ta₃/W₇ oxide (stearic acid, 1°C/min) for high acid value *Jatropha* oil (25.41 mg KOH/g) in the esterification reaction: 10:1 ratio of methanol to oil, 5 wt.% of the catalyst, and at 180°C for 2 h could give 75.10% conversion rate. Moreover, the reaction conditions reported in this work are much milder than those of WO₃/ZrO₂ (9:1 ratio of methanol to oil, 20 wt.% of the catalyst, and 150°C for 2 h) [22], SnO₂-SiO₂ (24:1 ratio of methanol to oil, 5 wt.% of the catalyst, and 180°C for 5 h) [23], and WO₃ (30 wt.%)/AlPO₄ (30:1 ratio of methanol to oil, 5 wt.% of the catalyst, and 180°C for 5 h) [24]. Under the optimal conditions, the mesoporous Ta₃/W₇ oxide (stearic acid, 1°C/min)

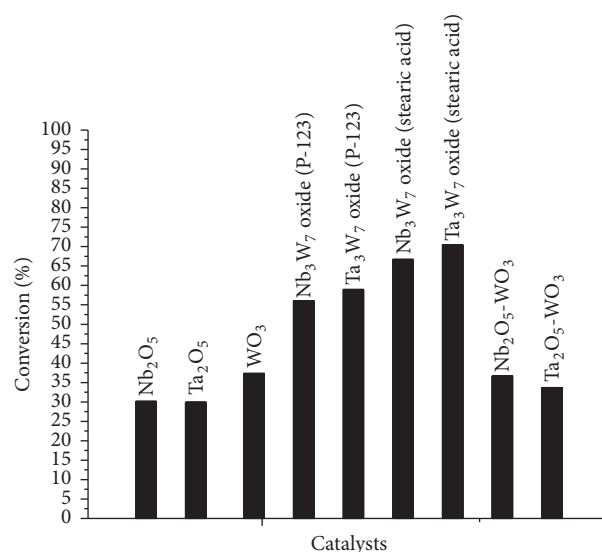


FIGURE 9: Effect of solid acid catalysts on the esterification reactions at 180°C.

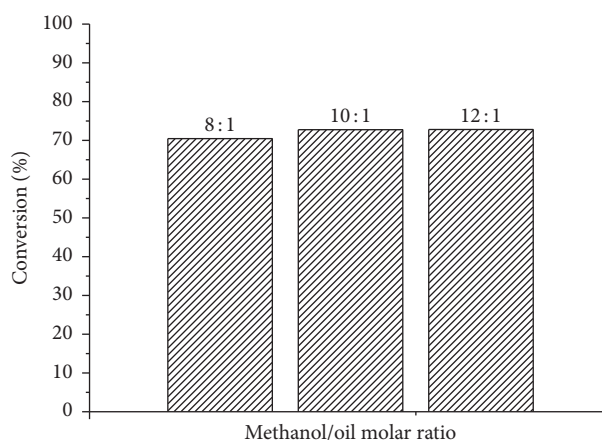


FIGURE 10: The influence of methanol to oil ratio on esterification reaction.

was used in the esterification reaction for the three plants oil: *Jatropha curcas* L. (9.34 mg KOH/g), *Euphorbia lathyris* L. (9.17 mg KOH/g), and *Sapium sebiferum* L. (4.89 mg KOH/g), the acid values of three natural oil were dropped by 2.09, 1.73, and 1.08 mg KOH/g, respectively, and the conversion rate

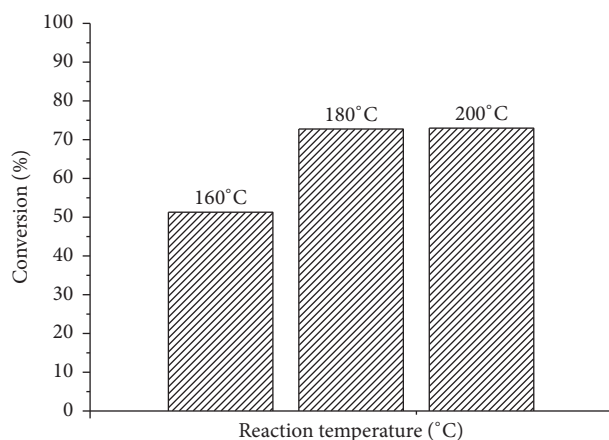


FIGURE 11: The influence of reaction temperature on esterification reaction.

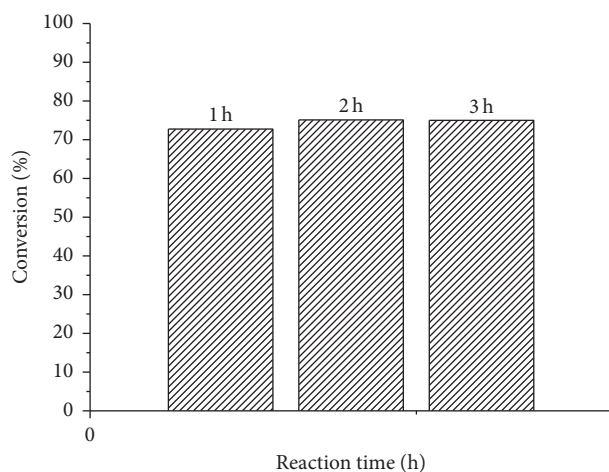


FIGURE 12: The influence of reaction time on esterification reaction.

was almost the same with the esterified high acid *Jatropha* oil (25.41 mg KOH/g).

3.3. Reusability of Catalyst. The reusability was an important key for the heterogeneous catalyst [25]. The recovered mesoporous Ta_3W_7 oxide (stearic acid, $1^\circ\text{C}/\text{min}$) was repeatedly washed with hexane, dried in vacuo, and calcined under the conditions of preparation of the fresh catalyst. Figure 13 shows the recycling results of the mesoporous Ta_3W_7 oxide (stearic acid) and Ta_3W_7 oxide (P123) catalyst in esterification reaction under the optimized reaction conditions. It was clearly found that these two catalysts could be reused for three times via regeneration, while the activity of Ta_3W_7 oxide (P123) (59.06%, 53.21%, 50.56%, 42.12%, and 35.17%) in five consecutive cycles was not as good as Ta_3W_7 oxide (stearic acid) (74.52%, 69.64%, 65.62%, 44.99%, and 37.08%). The change in physical properties of the catalyst after the reaction was proposed to result in the loss of the catalytic activity, based on a series of characterizations (Supporting information in Supplementary Material available online at <https://doi.org/10.1155/2017/9136528>).

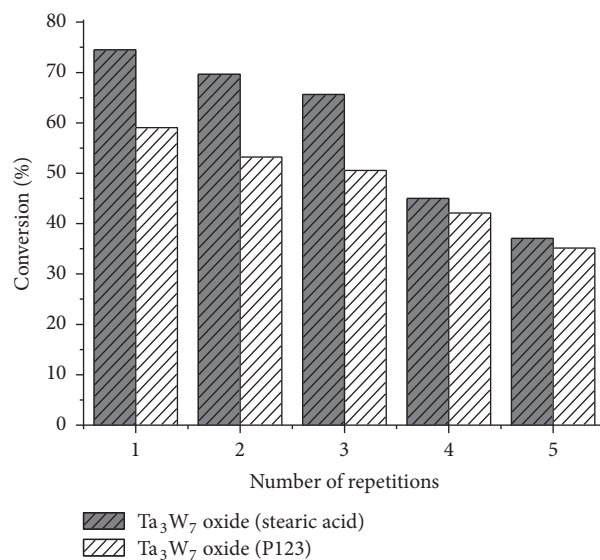


FIGURE 13: The reusability of mesoporous Ta_3W_7 oxide (stearic acid and P123).

4. Conclusions

In this study, we used the stearic acid instead of the expensive P-123 as the templates to prepare the solid acid catalysts Ta_3W_7 and Nb_3W_7 oxide of high activity, high surface areas, and mesopores by a thermal decomposition route. The surface area of both catalysts was $66.12 \text{ m}^2/\text{g}$ and $107.49 \text{ m}^2/\text{g}$, respectively. Compared with the preparation method of the mesoporous Ta_3W_7 and Nb_3W_7 oxide with P-123, this method shortened the preparation period from 15 days to 1 day and reduced 80% of cost. Among the catalysts, the mesoporous Ta_3W_7 oxides (stearic acid, $1^\circ\text{C}/\text{min}$) had the highest the specific surface area and high strength acid sites and showed the best catalytic activity in esterification of the high acid value *Jatropha* oil (acid value: 25.41 mg KOH/g). The acid value could be reduced from 25.41 to 5.52 mg KOH/g under the amount of catalyst 5 wt%, the molar ratio of methanol to oil 10 : 1, and the reaction at 180°C for 2 h. Furthermore, the catalyst was used to catalyze the *Jatropha curcas L.* oil, *Sapium sebiferum L.* oil, and *Euphorbia lathyris L.* oil with the acid value of 9.34 mg KOH/g, 9.17 mg KOH/g, and 4.89 mg KOH/g via esterification reaction, and the resulting product acid number dropped to 2.09 mg KOH/g, 1.73 mg KOH/g, and 1.08 mg KOH/g separately. Generally speaking, the modification method with the stearic acid could effectively improve the specific surface area and density of active sites of the solid acid catalyst and exhibit the high catalytic performance for the oil of high acid in esterification. Evaluations on the cost of industry and other related economics of the catalysts will be studied in our future work.

Competing Interests

The authors have no competing interests to declare.

Acknowledgments

This work was financially supported by the Natural Science Foundation of China (no. 21576059), Guizhou Provincial S&T Program (nos. SZ-[2009]3011, G[2008]7001, and [2009]2), and Guizhou Provincial, State, University S&T Joint Fund Program (no. LH [2015]7762).

References

- [1] H. Li, Z. Fang, R. L. Smith, and S. Yang, "Efficient valorization of biomass to biofuels with bifunctional solid catalytic materials," *Progress in Energy and Combustion Science*, vol. 55, pp. 98–194, 2016.
- [2] C.-Y. Lin, H.-A. Lin, and L.-B. Hung, "Fuel structure and properties of biodiesel produced by the peroxidation process," *Fuel*, vol. 85, no. 12–13, pp. 1743–1749, 2006.
- [3] F. Ma and M. A. Hanna, "Biodiesel production: a review," *Bioresource Technology*, vol. 70, no. 1, pp. 1–15, 1999.
- [4] M. Zabeti, W. M. A. Wan Daud, and M. K. Aroua, "Activity of solid catalysts for biodiesel production: a review," *Fuel Processing Technology*, vol. 90, no. 6, pp. 770–777, 2009.
- [5] J. Zhang, S. Chen, R. Yang, and Y. Yan, "Biodiesel production from vegetable oil using heterogenous acid and alkali catalyst," *Fuel*, vol. 89, no. 10, pp. 2939–2944, 2010.
- [6] M. Canakci and J. Van Gerpen, "Biodiesel production from oils and fats with high fatty acids," *Transactions of the ASAE*, vol. 44, pp. 1429–1436, 2001.
- [7] A. S. Ramadhas, S. Jayaraj, and C. Muraleedharan, "Biodiesel production from high FFA rubber seed oil," *Fuel*, vol. 84, no. 4, pp. 335–340, 2005.
- [8] A. Kumar Tiwari, A. Kumar, and H. Raheman, "Biodiesel production from *Jatropha* oil (*Jatropha curcas*) with high free fatty acids: an optimized process," *Biomass and Bioenergy*, vol. 31, no. 8, pp. 569–575, 2007.
- [9] H. J. Berchmans and S. Hirata, "Biodiesel production from crude *Jatropha curcas* L. seed oil with a high content of free fatty acids," *Bioresource Technology*, vol. 99, no. 6, pp. 1716–1721, 2008.
- [10] C. Tagusagawa, A. Takagaki, A. Iguchi et al., "Synthesis and catalytic properties of porous Nb–Mo oxide solid acid," *Catalysis Today*, vol. 164, no. 1, pp. 358–363, 2011.
- [11] C. Tagusagawa, A. Takagaki, A. Iguchi et al., "Highly active mesoporous Nb–W oxide solid-acid catalyst," *Angewandte Chemie—International Edition*, vol. 49, no. 6, pp. 1128–1132, 2010.
- [12] R. Wang, H. Li, F. Chang et al., "A facile, low-cost route for the preparation of calcined porous calcite and dolomite and their application as heterogeneous catalysts in biodiesel production," *Catalysis Science & Technology*, vol. 3, no. 9, pp. 2244–2251, 2013.
- [13] Y. Feng, B. He, Y. Cao et al., "Biodiesel production using cation-exchange resin as heterogeneous catalyst," *Bioresource Technology*, vol. 101, no. 5, pp. 1518–1521, 2010.
- [14] C. A. R. Melo Júnior, C. E. R. Albuquerque, J. S. A. Carneiro et al., "Solid-acid-catalyzed esterification of oleic acid assisted by microwave heating," *Industrial & Engineering Chemistry Research*, vol. 49, no. 23, pp. 12135–12139, 2010.
- [15] Y. M. Wang, Z. Y. Wu, Y. L. Wei, and J. H. Zhu, "In situ coating metal oxide on SBA-15 in one-pot synthesis," *Microporous and Mesoporous Materials*, vol. 84, no. 1–3, pp. 127–136, 2005.
- [16] S. J. Gregg and K. S. W. Sing, *Adsorption, Surface Area, & Porosity*, Academic Press, London, UK, 2nd edition, 1982.
- [17] Y.-M. Park, D.-W. Lee, D.-K. Kim, J.-S. Lee, and K.-Y. Lee, "The heterogeneous catalyst system for the continuous conversion of free fatty acids in used vegetable oils for the production of biodiesel," *Catalysis Today*, vol. 131, no. 1–4, pp. 238–243, 2008.
- [18] J. Dhainaut, J.-P. Dacquin, A. F. Lee, and K. Wilson, "Hierarchical macroporous–mesoporous SBA-15 sulfonic acid catalysts for biodiesel synthesis," *Green Chemistry*, vol. 12, no. 2, pp. 296–303, 2010.
- [19] D. M. Alonso, F. Vila, R. Mariscal, M. Ojeda, M. L. Granados, and J. Santamaría-González, "Relevance of the physicochemical properties of CaO catalysts for the methanolysis of triglycerides to obtain biodiesel," *Catalysis Today*, vol. 158, no. 1–2, pp. 114–120, 2010.
- [20] H. H. Mardhiah, H. C. Ong, H. H. Masjuki, S. Lim, and H. V. Lee, "A review on latest developments and future prospects of heterogeneous catalyst in biodiesel production from non-edible oils," *Renewable and Sustainable Energy Reviews*, vol. 67, pp. 1225–1236, 2017.
- [21] M. G. Kulkarni, R. Gopinath, L. C. Meher, and A. K. Dalai, "Solid acid catalyzed biodiesel production by simultaneous esterification and transesterification," *Green Chemistry*, vol. 8, no. 12, pp. 1056–1062, 2006.
- [22] Y.-M. Park, J. Y. Lee, S.-H. Chung et al., "Esterification of used vegetable oils using the heterogeneous WO_3/ZrO_2 catalyst for production of biodiesel," *Bioresource Technology*, vol. 101, no. 1, pp. S59–S61, 2010.
- [23] W. Xie, H. Wang, and H. Li, "Silica-supported tin oxides as heterogeneous acid catalysts for transesterification of soybean oil with methanol," *Industrial & Engineering Chemistry Research*, vol. 51, no. 1, pp. 225–231, 2012.
- [24] W. Xie and D. Yang, "Transesterification of soybean oil over WO_3 supported on AlPO_4 as a solid acid catalyst," *Bioresource Technology*, vol. 119, pp. 60–65, 2012.
- [25] H. Li, Z. Fang, J. Luo, and S. Yang, "Direct conversion of biomass components to the biofuel methyl levulinate catalyzed by acid-base bifunctional zirconia-zeolites," *Applied Catalysis B: Environmental*, vol. 200, pp. 182–191, 2017.

